Research Article Vol. 28, No. 4 / 17 February 2020 / Optics Express 5179
Optics EXPRESS

Multi-wavelength coherent random laser in bio-microfibers

ZHENDONG XIE,[1,5] KANG XIE,[1,5] TAOPING HU,[2] JIAJUN MA,[3] JUNXI ZHANG,[1] RUI MA,[4] XUSHENG CHENG,[1] JIANQUAN LI,[1] AND ZHIJIA HU[1,3,4,*]

[1]*Laboratory of Optical Fibers and Micro-nano Photonics, School of Instrument Science and Opto-electronics Engineering, Hefei University of Technology, Hefei, Anhui 230009, China*
[2]*College of Science, Nanjing Forestry University, Nanjing, Jiangsu 210037, China*
[3]*State Key Laboratory of Environmental Friendly Energy Materials, Southwest University of Science and Technology, Mianyang, Sichuan 621000, China*
[4]*Aston Institute of Photonic Technologies, Aston University, Birmingham B4 7ET, UK*
[5]*Zhendong Xie and Kang Xie contributed equally to this work*
[*]*zhijiahu@hfut.edu.cn*

Abstract: In this paper, pure silk protein was extracted from Bombyx mori silks and fabricated into a new kind of disordered bio-microfiber structure using electrospinning technology. Coherent random lasing emission with low threshold was achieved in the silk fibroin fibers. The random lasing emission wavelength can be tuned in the range of 33 nm by controlling the pump location with different scattering strengths. Therefore, the bio-microfiber random lasers can be a wide spectral light source when the system is doped with a gain or energy transfer medium with a large fluorescence emission band. Application of the random lasers of the bio-microfibers as a low-coherence light source in speckle-free imaging had also been studied.

1. Introduction

Traces of natural silks can be found in many places in our daily lives. The properties of natural silks differ. Some, such as Bombyx mori silks, have perfect bending flexibility and tensile strength, while others, such as spider silks, exhibit stickiness for purposes such as catching insects. After human processing, some natural silks can be fabricated into useful items in photonics, such as silk-based optical-fiber chemical sensors [1], biological optical fibers [2], or new broadband nonlinear optical materials [3]. In general, the most useful natural silks are Bombyx mori silks, which are mainly composed of sericin and degummed silks formed from proteins containing α-amino acids. There are differences between sericin and degummed silks in species of amino acids, molecular arrangement, and structure. Degummed silks are easy to process and possess excellent mechanical properties and biological characteristics, and thus they are mainly used in research [4]. Bombyx mori silks are the earliest known type of natural silk to be used by humans, and can be spun into clothing or made into silk fibroin solution after degumming, which is an essential process for rebuilding silks. Various optical structures made of silk protein materials, such as porous scaffolds, thin films, and microfibers, can be obtained through electrospinning technology [5]. Silk fibroin (SF) extracted from Bombyx mori cocoons can be used in many fields, such as photonics and medicine, due to its high biocompatibility of solution processing and tunability of the material properties [6]. Researchers have also explored the feasibility of SF in new flexible photonic and optical devices [7].

Random lasers (RLs) have been the subject of intense research owing to their easy fabrication, low coherence, and small size [8–17]. The lasing feedback mechanism is synergistically achieved by multiple light scattering, which is different from traditional lasers [18–27]. Generally, disordered systems containing gain medium and scattering particles are essential for the generation

#384105 https://doi.org/10.1364/OE.384105
Journal © 2020 Received 25 Nov 2019; revised 21 Jan 2020; accepted 21 Jan 2020; published 10 Feb 2020

Optics EXPRESS

of RLs [28]. Recently, some biological samples doped with laser dye have been used as a new form of RL gain medium. For example, RLs have been observed in organic–inorganic hybrids, which combine SF with inorganic materials [29]. Some reports have introduced RLs with Anderson light localization in nanofibrillar structures in silkworm silk fibers [30–32]. From all of these it can been seen that native silks have great potential in disorder photonics.

In this paper, we created a disordered bio-microfiber structure using electrospinning technology. The bio-microfibers were fabricated by electrospinning technology, which is capable of high-volume production. Compared with other methods to fabricate bio-microfibers, the length of electrospinning bio-microfibers is much longer than those in previous reports. Coherent RLs have been observed in this structure with a low threshold of 2.68 μJ. The wavelength of the RLs can be controlled by changing the pump position due to different scattering strengths, which will be applied in optical biosensors on chips and a multi-color RL. The tunable wavelength range was as wide as 33 nm (from 556 to 589 nm). Because the bio-RLs possess low spatial coherence, we can use them as a light source in speckle-free imaging to obtain images with very low speckle contrast. This achievement demonstrates the potential application of bio-RLs in the field of speckle-free imaging.

2. Method

2.1. Preparation of SF solution

SF was obtained from Bombyx mori silks using a previous method [33,34]. First, the sericin and impurities on the surface of the silks were removed for their low crystallinity. The Bombyx mori cocoons were cut into pieces, of which 2 g were added to 1 L of 0.02 mol/L Na_2CO_3 solution at 100 °C for 45 min. The sericin and degummed silks were separated. The silks were washed thoroughly with milli-Q water to obtain pure degummed silks, which were dried at room temperature for 2 days. Second, the degummed silks were dissolved in 9.3 mol/L LiBr in a proportion of 1:4 (w/v) of fibroin to LiBr at 60 °C for 5 h, and a pale yellow solution was obtained. Thirdly, each 20 mL sample of the pale yellow solution was dialyzed with 250 mL of milli-Q water in a beaker for 4 h. This process was repeated for two days to remove the LiBr. Lastly, the remaining solution was centrifuged at a speed of 2000 r/min. The supernatant (pure SF solution) was put into sample bottles and stored at 4 °C.

2.2. Preparing a spinning solution

Samples of the SF solution were put in petri dishes and dried at 45 °C for 5 h to form SF films. The SF films were grinded into powders, which were then dissolved into hexafluoroisopropanol (HFIP) in a proportion of 0.9% (w/w) of fibroin to HFIP. This process lasted for several days, as the SF does not easily dissolve. The laser dye Rh6G was added into the organic solution in a proportion of 0.5% (w/w) of dye to fibroin. As the Rh6G was completely dissolved, a spinning solution was formed.

2.3. Electrospinning SF

The electrospun bio-microfibers were fabricated from SF/HFIP solution using a specific electrospinning process. A commercial electrospinning system (Beijing Ucalery Technology, SS-2535H) was used to electrospin the SF solution at room temperature. A 2.5 mL measure of spinning solution was put into a syringe with a metal nozzle. Under continuous spinning in an electric field of 1.5 kV/cm for 5 min, the electrospun bio-microfibers were collected on the aluminum film.

2.4. Laser pumping and spectral acquisition

A Q-switched Nd:YAG laser that outputs a wavelength of 532 nm (pulse duration 10 ns, repetition rate 10 Hz) was used to pump the electrospun microfibers. A microscope measurement setup

Optics EXPRESS

was built based on the micro spectrum system (Ideaoptics) to obtain detailed experimental data. As shown in Fig. 1, the pump pulse energy and polarization are controlled by a Glan prism group. An attenuator is placed in the optical path to obtain a lower energy. The next two mirrors play the role of reflecting the pumping laser to change the laser path and guide the laser into the micro spectrum system. The pumping laser is reflected by a dichroic mirror and focused onto the samples via an objective. The samples on the objective table are excited by the 532 nm laser to generate fluorescence emission/random lasing. The emitted light is collected by the same objective and passed through a dichroic mirror with total transmission. The collected light is then focused onto a beam splitter via a concave lens, at which point 50% of the light is sent to a CCD camera to obtain an image of the samples. The other 50% of the light is directly collected with a fiber-coupled spectrometer (QE65PRO, Ocean Optics, resolution ~0.4 nm, integration time 100 ms). The CCD and spectrometer probes are conjugate surfaces, because the optical distances from the objective table to the faces of the CCD and spectrometer are equal.

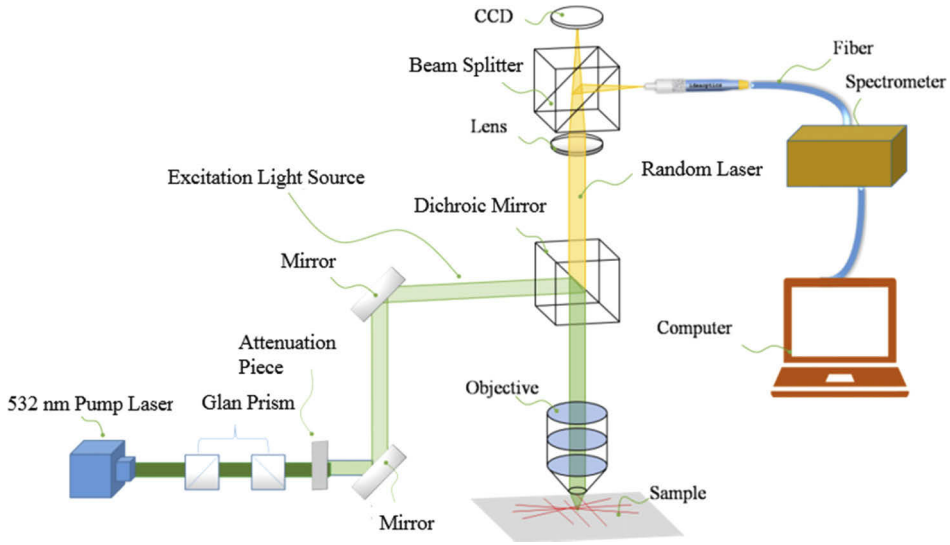

Fig. 1. Optical device diagram for bio-RLs. The energy of light passing through the mirror is modulated by a Glan prism group. A 10^{-1} attenuator is placed in the optical path to obtain a lower energy. A set of flat mirror reflectors guides the pump light into pumping the sample. The morphology of the sample is seen by the CCD camera and the spectra can be captured by the spectrometer above.

3. Results and discussion

3.1. Characterization of the electrospun microfibers

Figure 2(a) shows images of the electrospinning solution. The left image is the pure SF solution dissolved in HFIP. The right image is the SF solution mixed with laser dye Rh6G. The solution is pale yellow and turns yellow after mixing with Rh6G. Figures 2(b)–2(d) show SEM micrographs of the bio-microfibers with different scale bars. As illustrated in Fig. 2(b), which is magnified by a factor of 50, the bio-microfibers form a very dense network film. It can be seen from Fig. 2(c) that the directions of the bio-microfibers are random. Some of the bio-microfibers are straight, but some are tortuous, and this characterization enhances the inter-microfiber scattering. As shown in Fig. 2(d), the diameters of the bio-microfibers range from 0.1 μm to 1 μm and their surfaces are very smooth, which indicates that a single fiber can be used to transmit light. More importantly, the bio-microfibers are parallel to the plane of the aluminum film.

Optics EXPRESS

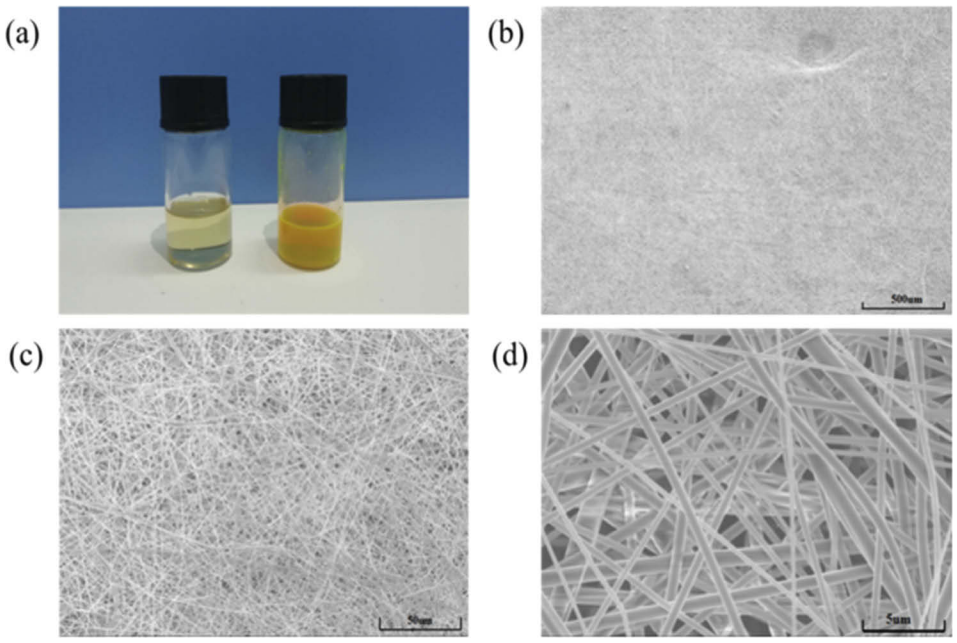

Fig. 2. (a) Imaging of pure SF solution and SF solution mixed with Rh6G; (b)–(d) SEM micrographs at different scale bars.

From the above analysis, the characteristics of the bio-microfibers perform well and are qualified to generate RLs. To obtain a high-quality sample, degumming is an essential process before electrospinning, because the sericin on the surface of Bombyx mori silks leads to a low crystallinity of electrospun bio-microfibers. Moreover, a proper proportion of fibroin to HFIP is also necessary for the formation of bio-microfibers.

3.2. Spectral characteristics of the electrospun microfibers

The random lasing emission spectra obtained from the microfibers mixed with Rh6G at different pump energies are shown in Fig. 3(a). Typical random lasing behavior with spiked peaks was observed, which indicates that resonant feedback has occurred in this structure. At a low pump energy of 1 μJ, there was no lasing emission. When the pump energy was over 2 μJ, random lasing appeared with very small spiked peaks. The spiked peaks represent specific laser modes, which are strong evidence of the generation of coherent random lasing. At the energy of 2 μJ, there was only one spiked peak. When the pump energy increased to 3 μJ, there was also one main emission peak, but there were also imperceptibly weak peaks around the main peak. The weak peaks became obvious at the energy of 5 μJ. The intensities of the peaks increased at the energy of 8 μJ. The insert of Fig. 3(a) is an enlarged view of the spectrum at the energy of 10 μJ, where there were eight peaks from 564 to 573 nm and the full width at half maximum (FWHM) reached as low as 0.4 nm at 567 nm. When the pump energy increased above 1 μJ, the number of spiked peaks increased. This indicates that there are more coherent loops to boost lasing modes. When the number of spiked peaks reached its maximum, the intensities of the peaks increased without new peaks emerging as the pump energy increased. From the relationship between input and output, as shown in Fig. 3(b), it can be seen that there is a nonlinear increment and the threshold is obtained as 2.68 μJ.

The scattering strength varies in different locations on the sample, which results in different random lasing emissions. As shown in Fig. 4, there are four random lasing spectra in different

Optics EXPRESS

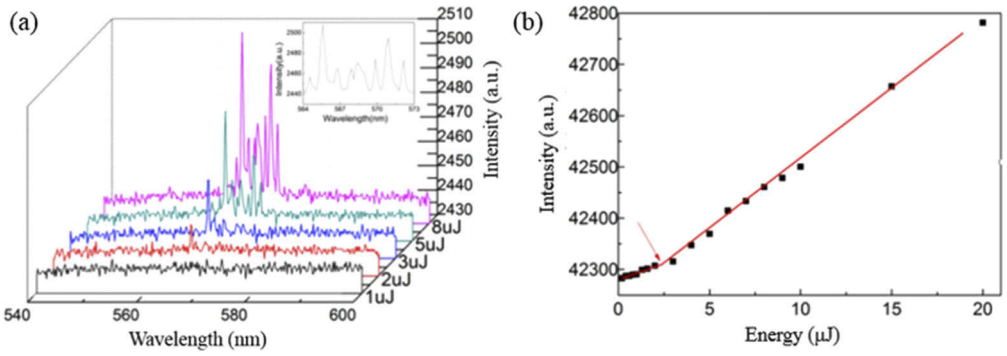

Fig. 3. (a) Evolution of random lasing spectra at different pump energies; (b) input–output relationship. Inset: random lasing spectrum at pump energy of 10 μJ.

pump locations under the pump energy of 10 μJ. Initially, the spectrum (red line) with lasing wavelength range from 564 to 568 nm was found when the pump light was moved with a random displacement distance. When the sample was moved to change the pump position, a different spectrum was found with lasing wavelength range from 576 to 589 nm, as shown by the pink line. There is a significant difference between the two spectra in lasing wavelength. This interesting phenomenon gave us the possibility to control the wavelength of bio-RLs by changing the pumping location. A large number of spectra were collected to change the pumping area. Four typical spectra are selected and shown in Fig. 4 after analyzing the collected spectra from different locations on the sample. As shown in Fig. 4 by the black line with lasing wavelength range from 556 to 561 nm, the smallest wavelength is 556 nm. The blue line with lasing wavelength range from 566 to 574 nm illustrates that the lasing wavelength is changed continuously. Two reasons are proposed for the different random lasing wavelengths in different pumping locations. The first reason is different arrangements of bio-microfibers in different locations, which causes different scattering paths, thus generating various random lasing wavelengths. The second reason is that the diameters of the different bio-microfibers are not uniform, which results in different thickness of laser gain. As mentioned above, the diameters of some bio-microfibers are as thick as 1 μm, but some are only as thick as 0.1 μm. This feature also introduces differences between the scattering paths. As the above analyses show, the tuning wavelength range in the bio-RL system is about 33 nm. This feature indicates that it is possible for the RLs to be used as a multi-color random laser.

To illustrate this clearly, Fig. 5 shows bio-RL images of the bio-microfibers and corresponding chromatogram from 550 to 600 nm. Figure 5(a) is the light image of bio-RLs shown by the black line in Fig. 4. The main emission color of the bio-RLs was green, which was consistent with the color of the corresponding chromatogram. The brightest part was in the center of the glowing area. Figure 5(b) is the light image of bio-RLs with wavelength range from 566 to 574 nm. As shown in the image, the emission color was green and yellow. The color of the chromatographic columns started to change from green to yellow as the wavelength shifted from 556 to 574 nm. The yellow parts were mainly located in the center, and the green light was seen at the edge of the yellow light. The most intense part of the light was slightly outward from the center, which was different from in the previous image. The light spot in Fig. 5(c) is formed completely by yellow light. The color of the wavelength range from 576 nm to 589 nm was already yellow. The bright parts of the picture formed a circle, and the intensity of light in the center was slightly weaker. Comparing the images of three different random lasing behaviors, we can observe the transmission of color from green to yellow. This is a powerful evidence for the feasibility of a multi-color RL. As the structures of the three images vary, it is proven that different disordered

Optics EXPRESS

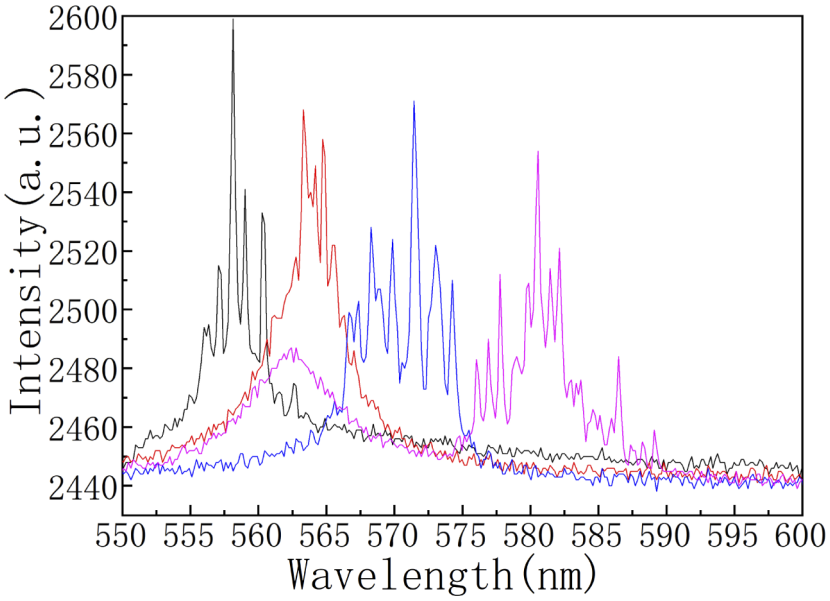

Fig. 4. Random lasing spectra at different pump positions.

structures can provide different feedbacks to the generation of RLs. This is why bio-RLs of different wavelengths can be obtained in different pumping areas in just one sample.

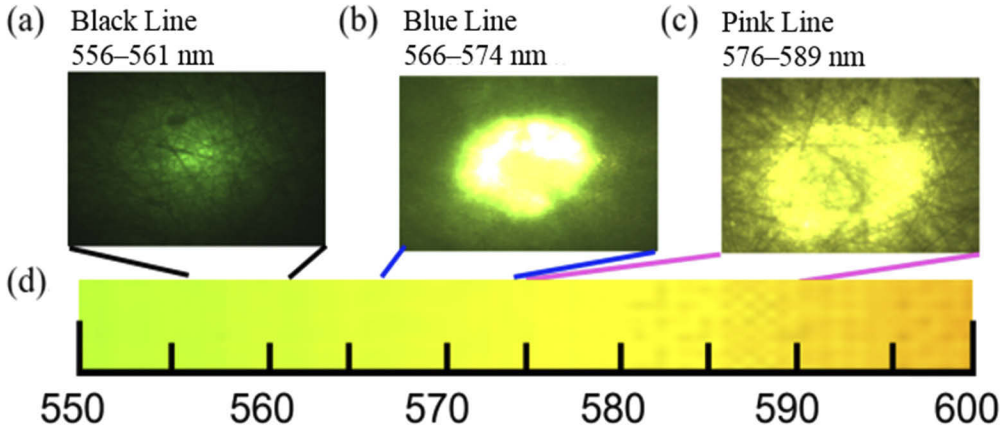

Fig. 5. (a)–(c) Imaging of structure with different random lasing emission wavelengths; (d) corresponding chromatogram from 550 to 600 nm.

Random lasing spectra for different random lasing emission wavelengths are shown in Fig. 6. The thresholds of the bio-RLs with wavelength ranges of 560–566 nm, 565–575 nm, 570–580 nm, and 570–589 nm were approximately 4, 5, 2, and 2 μJ, respectively. The thresholds for these cases were almost the same. There is no relationship between the threshold and these cases. The thresholds of the RLs showed fluctuation, and some of the bio-RLs had very low thresholds. These prevented us from studying the relationship between laser threshold and random lasing emission wavelength. The emission wavelength of RLs is related to both the thickness of the film and the arrays of bio-microfibers. If the film is thicker, the self-absorption will be stronger. The random lasing wavelength exhibits red-shift. The scattering intensity is strongly dependent on

Optics EXPRESS

the arrangements of the bio-microfibers. If the scattering becomes stronger, the wavelengths exhibit blue-shift. Because the structure of the bio-microfibers is very complicated, it is difficult to obtain and control the precise parameters of the thicknesses and arrays.

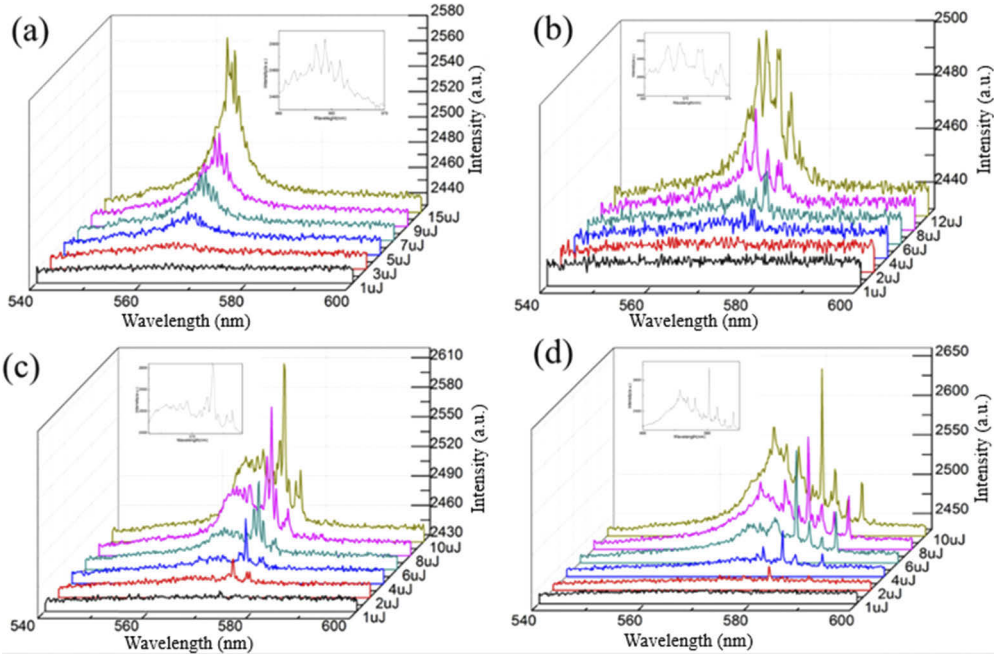

Fig. 6. Random lasing spectra for different wavelength. (a) the evolution of random lasing spectra with wavelength ranges of 560–566 nm; (b) 565–575 nm; (c) 570–580 nm; (d) 570–589 nm.

3.3. Spatial characteristics of the electrospun microfibers

Due to the low spatial coherence of RLs, there is an interesting opportunity for application in speckle-free optical imaging. Here, two kinds of laser lights were studied as imaging light sources: one was the pump light reflected from the electrospun bio-microfibers, which had a high degree of spatial coherence; the other was the bio-RLs generated from the bio-microfibers, which had a low degree of spatial coherence. Figure 7(a) shows the experimental setup for speckle-free imaging using the RLs generated from bio-microfibers as an illumination source. The sample was placed at 45° with respect to the pump light direction. The bio-RLs were passed through a filter to remove the pump light. The bio-RLs were focused onto the resolution chart by a lens. An opaque lens barrel was used to connect the objective lens and camera to avoid the effects of stray light. After adjusting the distance between the objective and resolution chart to image it on the camera, the light source with a high degree of spatial coherence created a speckle image, while the light source with a low degree of spatial coherence created a speckle-free image. Because the bio-RLs are scattered in all directions due to the cylindrical shape of the bio-microfibers, and the bio-microfibers themselves introduces random phase delay into the bio-RLs, the directions and phases are in random order, which causes the low spectral coherence. Figure 7(b) shows the speckle-free imaging under the illumination of the bio-RLs. Figure 7(c) shows the speckle imaging under the illumination of the pump light. Due to the low spatial coherence that allows speckle-free images to be obtained, bio-RLs perform well in this imaging system.

To analyze the spatial coherence, the speckle contrast C is defined as $\sigma_1/(I)$, where σ_1 is the standard deviation of the image intensity and I is the average intensity of the image. The

Optics EXPRESS

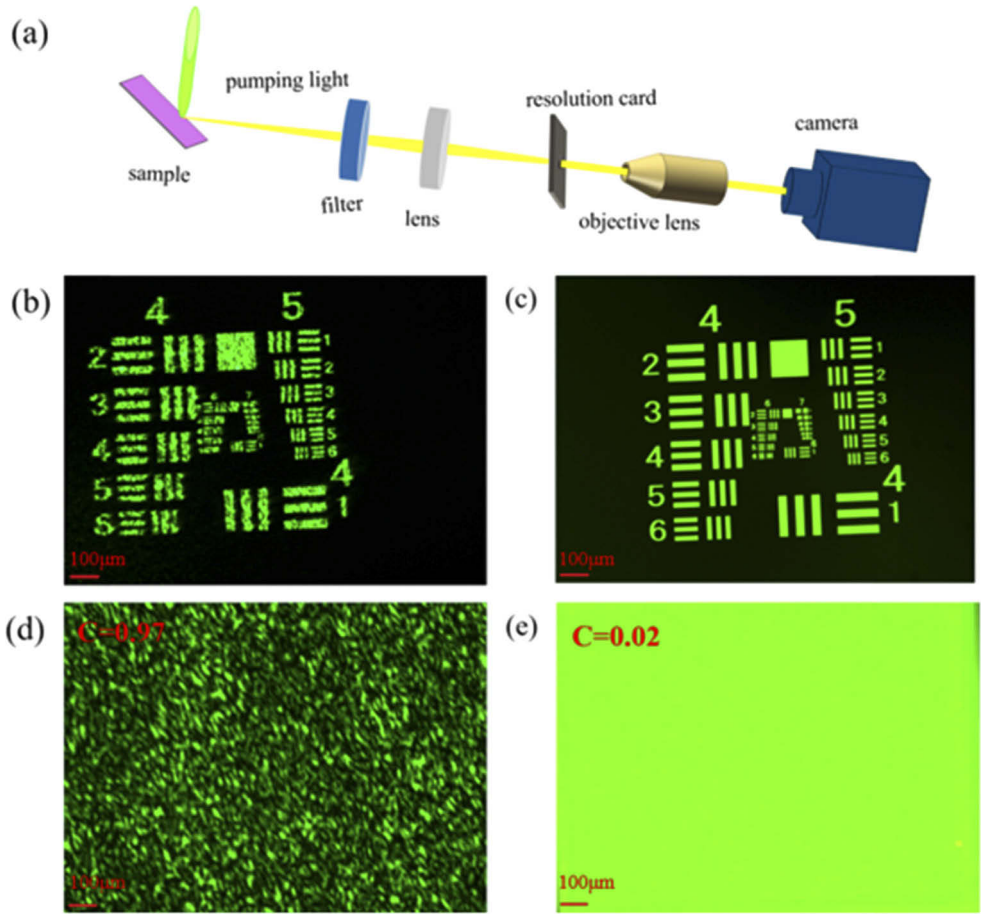

Fig. 7. (a) Experimental setup for speckle-free imaging using the electrospun microfibers as an illumination source; images of the resolution chart under the illumination of the (b) RLs and (c) pump light; and speckle contrast of the (d) pump light and (e) RLs.

situation in which the light has a speckle contrast of 1 indicates totally spatial coherent light, and that in which the light has a speckle contrast of 0 indicates that the light is totally spatial incoherent. Here, the speckle contrast of the bio-RLs (Fig. 7(e)) was 0.02, showing the low spatial coherence of the RLs. As shown in Fig. 7(e), there is speckle-free imaging caused by coherent light. The light intensity was very uniform. It can be seen that bio-RLs are the ideal light source for speckle-free imaging. In contrast, the pumping laser with very high spatial coherence (Fig. 7(d)) led to a very large speckle contrast of 0.97, which degraded the imaging quality as demonstrated in Fig. 7(b). From the above discussion, it is clear that the bio-RLs have great potential in speckle-free imaging.

4. Conclusion

Silk protein was extracted from Bombyx mori cocoons and mixed with Rh6G to obtain a spinning protein solution. Further, Bombyx mori silk was spun into a new disordered structure by the electrospinning technique. The bio-microfibers were arranged in all directions to form a disordered structure. Coherent RLs with wide ranges of wavelengths and low thresholds were observed in this complex disordered structure. The random lasing emission wavelength was tuned

Optics EXPRESS

within a range of 33 nm by controlling the pump location with different scattering strengths. RLs with a speckle contrast of 0.02 had been used as an illumination source for optical speckle-free imaging. From the results illustrated, it is clear that biological silks perform well in photonics.

Funding

National Natural Science Foundation of China (11404086, 11404087, 11574070, 11874012, 11874126, 51771186, 61501165); Fundamental Research Funds for the Central Universities (JZ2019HGPA0099, PA2018GDQT0006); Southwest University of Science and Technology (19FKSY0111); Anhui Province Key Laboratory of Environment-Friendly Polymer Materials (KF2019001); H2020 Marie Skłodowska-Curie Actions (744817); China Postdoctoral Science Foundation (2015M571917, 2017T100442).

Acknowledgments

Thanks to all the authors in this article for their efforts. In particular, thanks to Professor Hu for his guidance and the support of the Laboratory of Optical Fibers and Micro-nano Photonics of Hefei University of Technology.

References

1. K. H. Tow, D. M. Chow, F. Vollrath, I. Dicaire, T. Gheysens, and L. Thevenaz, "Exploring the use of native spider silk as an optical fiber for chemical sensing," J. Lightwave Technol. **36**(4), 1138–1144 (2018).
2. N. Huby, V. Vié, A. Renault, S. Beaufils, T. Lefèvre, F. Paquet-Mercier, M. Pézolet, and B. Bêche, "Native spider silk as a biological optical fiber," Appl. Phys. Lett. **102**(12), 123702 (2013).
3. B. Lee, H. Kwon, S. Kim, and F. Rotermund, "Natural silk protein as a new broadband nonlinear optical material," Opt. Mater. Express **6**(4), 993–1002 (2016).
4. B. Kundu and S. C. Kundu, "Osteogenesis of human stem cells in silk biomaterial for regenerative therapy," Prog. Polym. Sci. **35**(9), 1116–1127 (2010).
5. D. N. Rockwood, R. C. Preda, T. Yücel, X. Wang, M. L. Lovett, and D. L. Kaplan, "Materials fabrication from Bombyx mori silk fibroin," Nat. Protoc. **6**(10), 1612–1631 (2011).
6. H. Wang, Y. Chen, and Y. Zhang, "Processing and characterization of powdered silk micro- and nanofibers by ultrasonication," Mater. Sci. Eng., C **48**, 444–452 (2015).
7. M. B. Applegate, G. Perotto, D. L. Kaplan, and F. G. Omenetto, "Biocompatible silk step-index optical waveguides," Biomed. Opt. Express **6**(11), 4221–4227 (2015).
8. Y. Ling, H. Cao, A. L. Burin, M. A. Ratner, X. Liu, and R. P. H. Chang, "Investigation of random lasers with resonant feedback," Phys. Rev. A **64**(6), 063808 (2001).
9. Z. Hu, J. Xia, Y. Linag, J. Wen, E. Miao, J. Chen, S. Wu, X. Qian, H. Jiang, and K. Xie, "Tunable random polymer fiber laser," Opt. Express **25**(15), 18421–18430 (2017).
10. J. Xia, K. Xie, J. Ma, X. Chen, Y. Li, J. Wen, J. Chen, J. Zhang, S. Wu, X. Cheng, and Z. Hu, "The transition from incoherent to coherent random laser in defect waveguide based on organic/inorganic hybrid laser dye," Nanophotonics **7**(7), 1341–1350 (2018).
11. H. Cao, J. Y. Xu, E. W. Seelig, and R. P. H. Chang, "Microlaser made of disordered media," Appl. Phys. Lett. **76**(21), 2997–2999 (2000).
12. D. S. Wiersma, "The physics and applications of random lasers," Nat. Phys. **4**(5), 359–367 (2008).
13. B. Redding, M. A. Choma, and H. Cao, "Speckle-free laser imaging using random laser illumination," Nat. Photonics **6**(6), 355–359 (2012).
14. M. Leonetti, C. Conti, and C. López, "A random laser tailored by directional stimulated emission," Phys. Rev. A **85**(4), 043841 (2012).
15. Z. Hu, H. Zheng, L. Wang, X. Tian, T. Wang, Q. Zhang, G. Zou, Y. Chen, and Q. Zhang, "Random fiber laser of POSS solution-filled hollow optical fiber by end pumping," Opt. Commun. **285**(19), 3967–3970 (2012).
16. Z. Hu, Q. Zhang, B. Miao, Q. Fu, G. Zou, Y. Chen, Y. Luo, D. Zhang, P. Wang, H. Ming, and Q. Zhang, "Coherent random fiber laser based on nanoparticles scattering in the extremely weakly scattering regime," Phys. Rev. Lett. **109**(25), 253901 (2012).
17. L. Cerdán, A. Costela, I. García-Moreno, O. García, and R. Sastre, "Laser emission from mirrorless waveguides based on photosensitized polymers incorporating POSS," Opt. Express **18**(10), 10247–10256 (2010).
18. A. Costela, I. García-Moreno, D. del Agua, O. García, and R. Sastre, "Highly photostable solid-state dye lasers based on silicon-modified organic matrices," J. Appl. Phys. **101**(7), 073110 (2007).
19. Z. Hu, B. Miao, T. Wang, Q. Fu, D. Zhang, H. Ming, and Q. Zhang, "Disordered microstructure polymer optical fiber for stabilized coherent random fiber laser," Opt. Lett. **38**(22), 4644–4647 (2013).

Optics EXPRESS

20. N. Bachelard, S. Gigan, X. Noblin, and P. Sebbah, "Adaptive pumping for spectral control of random laser," Nat. Phys. **10**(6), 426–431 (2014).
21. N. Bachelard, J. Andreasen, S. Gigan, and P. Sebbah, "Taming random lasers through active spatial control of the pump," Phys. Rev. Lett. **109**(3), 033903 (2012).
22. T. Hisch, M. Liertzer, D. Pogany, F. Mintert, and S. Rotter, "Pump-controlled directional light emission from random lasers," Phys. Rev. Lett. **111**(2), 023902 (2013).
23. M. Leonetti, C. Conti, and C. López, "Non-locality and collective emission in disordered lasing," Light: Sci. Appl. **2**(8), e88 (2013).
24. M. Leonetti, C. Conti, and C. López, "Tunable degree of localization in random lasers with controlled interaction," Appl. Phys. Lett. **101**(5), 051104 (2012).
25. A. L. Burin, M. A. Ratner, H. Cao, and R. P. H. Chang, "Model for a random laser," Phys. Rev. Lett. **87**, 215503 (2001).
26. B. Fazio, A. Irrera, S. Pirotta, C. D'Andrea, S. Del Sorbo, M. J. Lo Faro, P. G. Gucciardi, M. A. Iatì, R. Saija, M. Patrini, P. Musumeci, C. S. Vasi, D. S. Wiersma, M. Galli, and F. Priolo, "Coherent backscattering of Raman light," Nat. Photonics **11**(3), 170–176 (2017).
27. S. Ferjani, A. De Luca, V. Barna, C. Versace, and G. Strangi, "Thermo-recurrent nematic random laser," Opt. Express **17**(3), 2042–2047 (2009).
28. Y. Sun, Z. Wang, X. Shi, Y. Wang, X. Zhao, S. Chen, J. Shi, J. Zhou, and D. Liu, "Coherent plasmonic random laser pumped by nanosecond pulses far from the resonance peak of silver nanowires," J. Opt. Soc. Am. B **30**(9), 2523–2528 (2013).
29. M. V. Santos, E. Pecoraro, S. H. Santagneli, A. L. Moura, M. Cavicchioli, V. Jerez, L. A. Rocha, L. F. C. de Oliveira, A. S. L. Gomes, C. B. de Araujo, and S. J. L. Ribeiro, "Silk fibroin as a biotemplate for hierarchical porous silica monoliths for random laser applications," J. Mater. Chem. **6**(11), 2712–2723 (2018).
30. B. Abaie, E. Mobini, S. Karbasi, T. Hawkins, J. Ballato, and A. Mafi, "Random lasing in an Anderson localizing optical fiber," Light: Sci. Appl. **6**(8), e17041 (2017).
31. S. H. Choi, S. W. Kim, Z. Ku, M. A. Visbal-Onufrak, S. R. Kim, K. H. Choi, H. Ko, W. Choi, A. M. Urbas, T. W. Goo, and Y. L. Kim, "Anderson light localization in biological nanostructures of native silk," Nat. Commun. **9**(1), 452 (2018).
32. S. Yang, S. Kim, H. Shin, S. H. Choi, Y. L. Kim, C. Joo, and W. Ryu, "Random lasing detection of structural transformation and compositions in silk fibroin scaffolds," Nano Res. **12**(2), 289–297 (2019).
33. A. Huot, T. Lefevre, J. F. Rioux-Dubé, F. Paquet-Mercier, A. P. Nault, M. Auger, and M. Pézolet, "Effect of mechanical deformation on the structure of regenerated Bombyx mori silk fibroin films as revealed using Raman and infrared spectroscopy," Appl. Spectrosc. **69**(6), 689–698 (2015).
34. Z. Huang, X. Liu, J. Wu, S. Wong, and J. Qu, "Electrospinning water harvesters inspired by spider silk and beetle," Mater. Lett. **211**, 28–31 (2018).